

Mixed Membership Distribution-Free Model

Huan Qing

QINGHUAN@CUMT.EDU.CN;QINGHUAN07131995@163.COM

School of Mathematics

China University of Mining and Technology

Xuzhou, 221116, P.R. China

Abstract

We consider the problem of detecting latent community information of mixed membership weighted networks in which nodes have mixed memberships and edge weights connecting between nodes can be finite real numbers. We propose a general mixed membership distribution-free model for this problem. The model has no distribution constraints of adjacency matrix's elements but only the expected values and can be viewed as generalizations of some previous models including the famous mixed membership stochastic blockmodels. Especially, signed networks in which nodes can belong to multiple communities can be generated from our model. We use an efficient spectral algorithm to estimate community memberships under the model. We derive the convergence rate of the proposed algorithm under the model using spectral analysis. We demonstrate the advantages of the mixed membership distribution-free model and the algorithm with applications to a small scale of simulated networks when adjacency matrix's elements follow different distributions. We have also applied the algorithm to five real-world weighted network data sets with encouraging results.

Keywords: Community detection, complex networks, distribution-free model, network analysis, overlapping weighted networks.

1. Introduction

For decades, the problem of community detection for networks has been actively studied in network science. The goal of community detection is to infer latent node's community information from the network, and community detection serves as a useful tool to learn network structure Fortunato (2010); Fortunato and Hric (2016); Papadopoulos et al. (2012). The classical Stochastic Block-model (SBM) (Holland et al., 1983) models non-mixed un-weighted networks by assuming that the probability of an edge between two nodes depends on their respective communities and each node only belongs to one community. Recent developments of SBM can be found in Abbe (2017). In real-world networks, nodes may have an overlapping property and belong to multiple communities Xie et al. (2013) while SBM can not model networks with overlapping property. The Mixed Membership Stochastic Blockmodel (MMSB) Airoldi et al. (2008) extends SBM by allowing nodes to belong to multiple communities. Models proposed in Karrer and Newman (2011); Jin et al. (2017); Zhang et al. (2020) extend SBM and MMSB by introducing node variation to model network in which node degree varies. Based on SBM and its extensions, substantial works on algorithms, applications and theoretical guarantees have been developed, to name a few, Rohe et al. (2011); Choi et al. (2011); Zhao et al. (2012); Lei and Rinaldo (2015); Abbe and Sandon (2015); Jin (2015); Joseph and Yu (2016); Abbe et al. (2016); Hajek et al. (2016); Gao et al. (2017); Chen et al. (2018); Zhou and A.Amini (2019); Wang et al. (2020); Mao et al. (2020).

However, the above models are built for un-weighted networks and they can not model weighted networks. To model weighted networks in which node only belongs to one community, some models which can be viewed as extensions of SBM are proposed Aicher et al. (2015); Jog and Loh (2015); Palowitch et al. (2018); Xu et al. (2020); Ng and Murphy (2021); Qing (2021, 2022b) in recent years. However, these models can not model weighted networks in which nodes may belong to multiple communities. Especially, the Distribution-Free Models (DFM) of Qing (2021) can model weighted networks without edge weights distribution constraint and allows spectral clustering to fit the model. Though the multi-way blockmodels proposed in Airoldi et al. (2013) can model mixed

membership weighted networks, it has a strong requirement on the distribution of edges such that edge weights must be random variables generated from Normal distribution. To model mixed membership weighted networks, this article proposes a model based on a combination of the stochastic block idea of Holland et al. (1983), the mixed membership idea introduced in Airoldi et al. (2008), and the distribution-free idea introduced in Qing (2021).

The main contributions of this work include:

(1) We provide a general Mixed Membership Distribution-Free (MMDF for short) model to model mixed membership weighted network in which nodes may belong to multiple communities and edge weight can be any finite real number. MMDF does not require any prior knowledge on any specific distribution of edge weights (we also use adjacency matrix's elements to denote edge weights occasionally) but only an expected value reflecting the community membership information, where the expected value is directly related to the structure of the proposed model. Especially, signed networks in which nodes can belong to multiple communities can be generated from MMDF. We also provide the identifiability of MMDF. Meanwhile, MMDF can be seen as extensions of some previous models such as SBM, MMSB, and DFM. Detailed comparisons of our MMDF with some previous models for un-weighted networks or weighted networks can be found in Table 1. To the best of our knowledge, our MMDF is the first model for mixed membership weighted networks in which edge weights can be generated from arbitrary distribution.

(2) We use a spectral algorithm to fit MMDF, where the algorithm is designed based on the simplex structure inherent in the eigendecomposition of the adjacency matrix. The theoretical consistency of the proposed algorithm is built under MMDF. Especially, theoretical results when elements of the adjacency matrix follow some distinct distributions can be immediately obtained from our results. When MMDF degenerates to SBM, we can obtain the classical separation condition of a standard network and this guarantees the optimality of our theoretical studies.

(3) We study the numerical performance of the proposed algorithm under MMDF when edge weights are generated from different distributions by changing some model parameters. The numerical results are consistent with our theoretical findings. We also apply the algorithm to five real-world social weighted networks, and our data analysis results reveal the difference in network purity for different weighted networks.

Notations. We take the following general notations in this article. Write $[m] := \{1, 2, \dots, m\}$ for any positive integer m . For a vector x and fixed $q > 0$, $\|x\|_q$ denotes its l_q -norm, and we drop q for $\|x\|_q$ when q is 2. For a matrix M , M' denotes the transpose of the matrix M , $\|M\|$ denotes the spectral norm, $\|M\|_F$ denotes the Frobenius norm, $\|M\|_{2 \rightarrow \infty}$ denotes the maximum l_2 -norm of all the rows of M , and $\|M\|_\infty := \max_i \sum_j |M(i, j)|$ denotes the maximum absolute row sum of M . Let $\text{rank}(M)$ denote the rank of matrix M . Let $\sigma_i(M)$ be the i -th largest singular value of matrix M , $\lambda_i(M)$ denote the i -th largest eigenvalue of the matrix M ordered by the magnitude, and $\kappa(M)$ denote the condition number of M . $M(i, :)$ and $M(:, j)$ denote the i -th row and the j -th column of matrix M , respectively. $M(S_r, :)$ and $M(:, S_c)$ denote the rows and columns in the index sets S_r and S_c of matrix M , respectively. For any matrix M , we simply use $Y = \max(0, M)$ to represent $Y_{ij} = \max(0, M_{ij})$ for any i, j . $\mathbf{1}$ is a column vector with all entries being ones. e_i is the indicator vector with a 1 in entry i and 0 in all others.

2. The Mixed Membership Distribution-Free model

Consider an undirected weighted network \mathcal{N} with n nodes $\{1, 2, \dots, n\}$. Let $A \in \mathbb{R}^{n \times n}$ be the symmetric adjacency matrix of \mathcal{N} such that $A(i, j)$ denotes the weight between node i and node j for $i, j \in [n]$, and A is called adjacency matrix in this article. As a convention, we do not consider self edges, so A 's diagonal elements are 0. Note that $A(i, j)$ can be 0, 1, or some other finite real numbers since \mathcal{N} is a weighted network in this article. We assume all nodes in \mathcal{N} belong to K perceivable communities

$$\mathcal{C}^{(1)}, \mathcal{C}^{(2)}, \dots, \mathcal{C}^{(K)}. \quad (1)$$

Since we consider mixed membership weighted network in this article, a node in \mathcal{N} may belong to multiple communities with different weights. Let $\Pi \in \mathbb{R}^{n \times K}$ be nodes membership matrix such that for $i \in [n], k \in [K]$,

$$\text{rank}(\Pi) = K, \Pi(i, k) \geq 0, \sum_{l=1}^K \Pi(i, l) = 1, \quad (2)$$

$$\text{Each of the } K \text{ communities has at least one pure node,} \quad (3)$$

where we call node i ‘pure’ if $\Pi(i, :)$ degenerates (i.e., one entry is 1, all others $K-1$ entries are 0) and ‘mixed’ otherwise. In Eq (2), since $\Pi(i, k)$ is the weight of node i on community $\mathcal{C}^{(k)}$, $\|\Pi(i, :)\|_1 = 1$ means that $\Pi(i, :)$ is a $1 \times K$ probability mass function (PMF) for node i . Eq (3) is important for the identifiability of our model. For convenience, call Eq (3) pure nodes condition. For model modeling networks with mixed memberships, the pure nodes condition is significant for model identifiability, see models for the un-weighted networks with mixed memberships considered in Jin et al. (2017); Mao et al. (2020); Zhang et al. (2020). Let \mathcal{I} be the indices of nodes corresponding to K pure nodes, one from each community. Without loss of generality, let $\Pi(\mathcal{I}, :) = I_K$, where I_K is the $K \times K$ identity matrix.

Let the $K \times K$ connectivity matrix P satisfy

$$P = P', \text{rank}(P) = K, \text{and } \max_{k, l \in [K]} |P(k, l)| = 1. \quad (4)$$

We’d emphasize that P may have negative elements, the full rank requirement of P is mainly for the identifiability of our model, and we set the maximum absolute value of P ’s entries as 1 mainly for convenience. Since P can have negative elements, it is not a matrix with probabilities unless \mathcal{F} is Bernoulli or Poisson or some other distributions. Meanwhile, unless specified, throughout this article, K is assumed to be a known integer.

Let $\rho > 0$ be a parameter that controls the sparsity of network \mathcal{N} , and call it sparsity parameter. For *arbitrary distribution* \mathcal{F} and all pairs of (i, j) with $i, j \in [n]$, our model constructs the adjacency matrix of the undirected weighted network \mathcal{N} such that $A(i, j)$ are independent random variables generated from \mathcal{F} with expectation

$$\mathbb{E}[A(i, j)] = \Omega(i, j), \text{ where } \Omega := \rho \Pi P \Pi'. \quad (5)$$

Call Ω population adjacency matrix in this article. Eq (5) means that we only assume all elements of A are independent random variables generated from the arbitrary distribution \mathcal{F} with expectation $\Omega(i, j)$, without any prior knowledge on a specific distribution of $A(i, j)$ for $i, j \in [n]$, and this guarantees that our model can model both weighted and un-weighted networks with mixed memberships. For comparison, mixed membership models considered in Airoldi et al. (2008); Zhang et al. (2020); Jin et al. (2017); Mao et al. (2018, 2020) require all entries of A are random variables from Bernoulli distribution with expectation $\Omega(i, j)$ since these models only model un-weighted networks.

Definition 1 *Call Equations (1)-(5) the Mixed Membership Distribution-Free (MMDF) model and denote it by $MMDF_n(K, P, \Pi, \rho)$.*

Next proposition which is distribution-free guarantees the identifiability of MMDF.

Proposition 1 *(Identifiability). MMDF is identifiable: For eligible (P, Π) and $(\tilde{P}, \tilde{\Pi})$, if $\rho \Pi P \Pi' = \rho \tilde{\Pi} \tilde{P} \tilde{\Pi}'$, then $\Pi = \tilde{\Pi}$ and $P = \tilde{P}$.*

All proofs of proposition, lemmas, and theorems are provided in the supplementary material in this paper. MMDF includes some previous models for community detection as special cases.

- Compared with the MMSB proposed in Airoldi et al. (2008), MMDF has no constraint on distribution \mathcal{F} and the distribution of Π while MMSB requires all entries of A follow Bernoulli distribution and Π follows Dirichlet distribution, and these increase the applicability of our

model. Especially, MMSB limits all elements of P to being nonnegative while our MMDF allows P to have negative entries. To conclude, our MMDF can model both weighted and un-weighted networks while MMSB only models un-weighted networks, i.e., MMSB is a sub-model of our MMDF.

- Compared with the model DFM, our MMDF reduces to DFM when all $\Pi(i, :)$ are degenerate, i.e., all nodes are pure. Thus, MMDF allows nodes to belong to multiple communities while DFM requires that each node belongs to a single community. Meanwhile, both MMDF and DFM can model weighted and un-weighted networks. To conclude, MMDF is a direct extension of DFM by allowing nodes to have mixed memberships, and the relationship between MMDF and DFM is similar as that of MMSB and SBM. Sure, our MMDF is also an extension of SBM since MMSB and DFM are extensions of SBM. It should be emphasized that though MMDF is an extension of DFM from a non-mixed membership network to a mixed membership network, it is at the cost of a stronger requirement on the rank of P for the model’s identifiability: MMDF’s identifiability requires P to be full rank while DFM’s identifiability allows P to be a singular matrix. And such a phenomenon also occurs for MMSB and SBM.
- Compared with the weighted MMSB (WMMSB) of Dulac et al. (2020), our MMDF has no limit on distribution \mathcal{F} , distribution of Π , and allows P to have negative entries, while WMMSB requires that A follows Poisson distribution, Π follows Dirichlet distribution, and all entries of P are nonnegative. Our MMDF is more general than WMMSB, i.e., WMMSB is a sub-model of our MMDF.
- Compared with weighted stochastic blockmodels (WSBM) in Aicher et al. (2015); Jog and Loh (2015); Palowitch et al. (2018); Xu et al. (2020); Ng and Murphy (2021), these WSBM model weighted network in which every node only belongs to one community, and some of them require all elements of P to be nonnegative, or some of them require P to only have two distinct elements, or they need some distribution constraints on A , while our MMDF is distribution-free, models weighted network in which nodes enjoy mixed memberships, and allows P to have negative entries.

Table 1 summarizes comparisons of our MMDF with some previous models.

Model	A	Distribution \mathcal{F}	Overlapping
SBM Holland et al. (1983)	$A \in \{0, 1\}^{n \times n}$	Bernoulli	No
MMSB Airolti et al. (2008)	$A \in \{0, 1\}^{n \times n}$	Bernoulli	Yes
DCSBM Karrer and Newman (2011)	$A \in \{0, 1\}^{n \times n}$	Bernoulli	No
OSBM Latouche et al. (2011)	$A \in \{0, 1\}^{n \times n}$	Bernoulli	No
Multi-way blockmodels Airolti et al. (2013)	$A \in \mathbb{R}^{n \times n}$	Normal or Bernoulli	Yes
WSBM Aicher et al. (2015)	$A \in \mathbb{R}^{n \times n}$	Exponential family	No
WSBM Jog and Loh (2015)	$A \in \mathbb{R}^{n \times n}$	arbitrary	No
OCCAM Zhang et al. (2020)	$A \in \{0, 1\}^{n \times n}$	Bernoulli	Yes
DCMM Jin et al. (2017)	$A \in \{0, 1\}^{n \times n}$	Bernoulli	Yes
WSBM Palowitch et al. (2018)	$A \in \mathbb{R}_+^{n \times n}$	Distributions defined on \mathbb{R}_+	No
WSBM Xu et al. (2020)	$A \in \mathbb{R}^{n \times n}$	arbitrary	No
WMMSB Dulac et al. (2020)	$A \in \mathbb{Z}_+^{n \times n}$	Poisson	Yes
WSBM Ng and Murphy (2021)	$A \in \mathbb{R}_+^{n \times n}$	Gamma	No
DFM Qing (2021)	$A \in \mathbb{R}^{n \times n}$	arbitrary	No
DCDFM Qing (2022b)	$A \in \mathbb{R}^{n \times n}$	arbitrary	No
MMDF (this article)	$A \in \mathbb{R}^{n \times n}$	arbitrary	Yes

Table 1: Summary of general comparisons of MMDF with previous models.

3. A spectral algorithm DFSP for fitting MMDF

The goal of community detection under model MMDF is to recover the membership matrix Π with network \mathcal{N} ’s adjacency matrix A and the known number of communities K . To estimate Π with

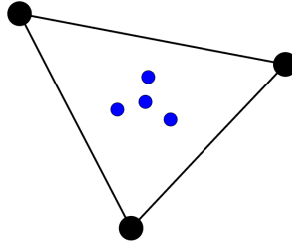


Figure 1: Rows of U : Ideal Simplex in Experiments 1-7 (black: pure nodes; blue: mixed nodes. Each point is a row of U . Many rows are equal by Lemma 1, so a point may denote many rows) of Section 5. K is 3, so there are three black points. Each PMF of mixed nodes belongs to 4 different PMFs, so there are 4 blue points. Since $K = 3$, for visualization, we have projected and rotated these points from \mathbb{R}^3 to \mathbb{R}^2 .

given A and K under MMDF, we start by providing an intuition on designing a spectral algorithm to fit model MMDF from the oracle case when Ω is known.

Since $\text{rank}(P) = K, \text{rank}(\Pi) = K, \text{rank}(\Omega) = K$ by basic algebra under $MMDF_n(K, P, \Pi, \rho)$. Let $\Omega = U\Lambda U'$ be the compact eigendecomposition of Ω such that $U \in \mathbb{R}^{n \times K}, \Lambda \in \mathbb{R}^{K \times K}$, and $U'U = I_K$. The following lemma functions similar as Lemma 2.1 of Mao et al. (2020) and guarantees the existence of Ideal Simplex (IS for short), and the form $U = \Pi B$ is called IS when Π satisfies Equation (2)). It should be emphasized that the existence of IS is distribution-free as long as Π satisfies Equations (2) and (3), and P is full rank.

Lemma 1 (*Ideal Simplex*). *Under $MMDF_n(K, P, \Pi, \rho)$, there exists an unique $K \times K$ matrix B such that $U = \Pi B$ where $B = U(\mathcal{I}, :)$.*

Figure 1 shows the IS by plotting rows of U under the settings in our simulations studies. We see that when i is a pure node, $U(i, :)$ is the vertex of IS; otherwise, $U(i, :)$ is in the interior of the IS, and this is consistent with Lemma 1.

Given Ω and K , we can compute U immediately by the top K eigendecomposition of Ω . Then, once we can obtain $U(\mathcal{I}, :)$ from U , we can exactly recover Π by $\Pi = UU^{-1}(\mathcal{I}, :)$ since $U(\mathcal{I}, :) \in \mathbb{R}^{K \times K}$ is a full rank matrix based on Lemma 1. As suggested by Jin et al. (2017); Mao et al. (2020), for such IS, we can take the advantage of the successive projection (SP) algorithm proposed in Gillis and Vavasis (2015) (i.e., Algorithm 2) to U with K communities to exactly find the corner matrix $U(\mathcal{I}, :)$. For convenience, set $Z = UU^{-1}(\mathcal{I}, :)$. Since $\Pi = Z$, we have $\Pi(i, :) = Z(i, :) \equiv \frac{Z(i, :)}{\|Z(i, :)\|_1}$ by the fact that $\|\Pi(i, :)\|_1 = 1$ for $i \in [n]$, where we write $\Pi(i, :) \equiv \frac{Z(i, :)}{\|Z(i, :)\|_1}$ mainly for the convenience to transfer the ideal algorithm given below to the real case.

The above gives rise to the following algorithm called Ideal DFSP (short for Distribution-Free SP algorithm), which is the ideal case of the SPACL algorithm proposed in Mao et al. (2020). Input Ω, K . Output: Π .

- Let U be the top K eigenvectors with unit-norm of Ω .
- Run SP algorithm on all rows of U with K communities to obtain \mathcal{I} .
- Set $Z = UU^{-1}(\mathcal{I}, :)$.
- Recover Π by $\Pi(i, :) = Z(i, :)/\|Z(i, :)\|_1$ for $i \in [n]$.

Given U and K , since the SP algorithm returns \mathcal{I} , we see that Ideal DFSP exactly returns Π , which supports the identifiability of MMDF in turn.

Next, we aim to extend the ideal case to the real case. The community membership matrix Π is unknown, and we aim at predicting it with given (A, K) when A is a random matrix generated from the arbitrary distribution \mathcal{F} under MMDF. Let $\hat{A} = \hat{U}\hat{\Lambda}\hat{U}'$ be the top K eigendecomposition of the adjacency matrix A such that $\hat{U} \in \mathbb{R}^{n \times K}$, $\hat{\Lambda} \in \mathbb{R}^{K \times K}$, $\hat{U}'\hat{U} = I_K$, and $\hat{\Lambda}$ contains the leading K eigenvalues of A . Algorithm 1 called DFSP is a natural extension of the Ideal DFSP to the real case, and DFSP is the SPACL algorithm without the prune step of Mao et al. (2020), where we re-name it as DFSP to stress the distribution-free property of this algorithm.

Remark 1 *DFSP can also obtain assignments to non-overlapping communities by setting $\hat{c}_i = \arg \max_{1 \leq k \leq K} \hat{\Pi}(i, k)$ for $1 \leq i \leq n$, where \hat{c}_i is the home base community that node i belongs to.*

Algorithm 1 DFSP

Require: The adjacency matrix $A \in \mathbb{R}^{n \times n}$ and the number of communities K .

Ensure: The estimated $n \times K$ membership matrix $\hat{\Pi}$.

- 1: Compute $\hat{A} = \hat{U}\hat{\Lambda}\hat{U}'$, the top K eigendecomposition of A .
 - 2: Run SP algorithm (i.e., Algorithm 2) on all rows of \hat{U} with K communities to obtain the estimated index set $\hat{\mathcal{I}}$ returned by SP.
 - 3: Set $\hat{Z} = \hat{U}\hat{U}^{-1}(\hat{\mathcal{I}}, :)$. Then set $\hat{Z} = \max(0, \hat{Z})$.
 - 4: Estimate $\Pi(i, :)$ by $\hat{\Pi}(i, :) = \hat{Z}(i, :)/\|\hat{Z}(i, :)\|_1$, $i \in [n]$.
-

The time cost of DFSP mainly comes from the eigendecomposition step and SP step. The computational cost of top K eigendecomposition is $O(Kn^2)$ and the computational cost of SP is $O(nK^2)$ Jin et al. (2017). Because $K \ll n$ in this paper, as a result, the total computational complexity of DFSP is $O(Kn^2)$. In Section 6, DFSP processes a real-world weighted network up to 27519 nodes within 40 seconds.

4. Asymptotic consistency of DFSP under MMDF

In this section, we aim at proving that the estimated membership matrix $\hat{\Pi}$ returned by DFSP concentrates around Π when A is a random matrix generated under MMDF for any distribution F . We need the following two assumptions to control the variances of all entries of A and the sparsity of network \mathcal{N} .

Assumption 1 *Assume*

- $\tau = \max_{i, j \in [n]} |A(i, j) - \Omega(i, j)|$ is finite.
- $\gamma = \frac{\sigma_A^2}{\rho}$ is finite, where $\sigma_A^2 = \max_{i, j \in [n]} \text{Var}(A(i, j))$ and $\text{Var}(A(i, j))$ denotes the variance of $A(i, j)$.

Assumption 2 *Assume $\gamma\rho n \geq \tau^2 \log(n)$.*

Assumption 1 is mild since it just requires that all entries of A and Ω and all variances of A 's elements are finite. When A is generated from some distributions under MMDF such that all elements of A are nonnegative, Assumption 2 means a lower bound requirement on network sparsity since ρ controls network sparsity when $A \in \mathbb{R}_+^{n \times n}$. However, when there exist some negative values in A , Assumption 2 means a lower bound requirement on network size for theoretical analysis. For details on γ 's finiteness and Assumption 2 under different distribution \mathcal{F} , see Examples 1-6.

Similar to Jin et al. (2017); Mao et al. (2018, 2020), main theoretical results on bounds of errors for estimating mixed memberships rely on row-wise eigenspace error between the eigenvectors of the adjacency matrix and eigenvectors of the population adjacency matrix. With applications of Theorem 1.4 (the Matrix Bernstein) in Tropp (2012) and Theorem 4.2 in Cape et al. (2019) where these two theorems are distribution-free, the next lemma provides an upper bound of row-wise eigenspace error.

Lemma 2 (*Row-wise eigenspace error*) Under $MMDF_n(K, P, \Pi, \rho)$, when assumptions 1 and 2 hold, suppose $\sigma_K(\Omega) \geq C\sqrt{\gamma\rho n \log(n)}$ for some $C > 0$, with probability at least $1 - o(n^{-3})$, we have

$$\|\hat{U}\hat{U}' - UU'\|_{2 \rightarrow \infty} = O\left(\frac{\sqrt{\gamma n \log(n)}}{\sigma_K(P)\rho^{0.5}\lambda_K^{1.5}(\Pi'\Pi)}\right).$$

Though γ is assumed to be finite by assumption 1, we still let it enter the bound in Lemma 2 since it is directly related to the variances of A 's elements under distribution \mathcal{F} , i.e., γ is related with distribution \mathcal{F} in our theoretical analysis though our model MMDF has no constraint on a specific distribution \mathcal{F} as long as Eq (5) holds. Meanwhile, we also benefit a lot from letting γ enter the theoretical bound when we aim at studying DFSP's performance under different distributions, and discussions after Corollary 1 support this statement. Alternatively, Theorem 4.2. of Chen et al. (2021) can also be applied to obtain the upper bound of $\|\hat{U}\hat{U}' - UU'\|_{2 \rightarrow \infty}$, and this bound is similar as the one in Lemma 2. For convenience, set $\varpi = \|\hat{U}\hat{U}' - UU'\|_{2 \rightarrow \infty}$. With an application of Lemma 2, the next theorem provides a theoretical upper bound on the l_1 errors of estimations for node memberships under MMDF.

Theorem 1 Under $MMDF_n(K, P, \Pi, \rho)$, let $\hat{\Pi}$ be obtained from DFSP algorithm, suppose conditions in Lemma 2 hold, there exists a permutation matrix $\mathcal{P} \in \mathbb{R}^{K \times K}$ such that with probability at least $1 - o(n^{-3})$, we have

$$\max_{i \in [n]} \|e'_i(\hat{\Pi} - \Pi\mathcal{P})\|_1 = O(\varpi\kappa(\Pi'\Pi)\sqrt{\lambda_1(\Pi'\Pi)}).$$

Since our model MMDF is distribution-free and \mathcal{F} can be arbitrary distribution as long as Eq (5) holds, Theorem 1 provides a general theoretical upper bound of the l_1 error between the estimated membership matrix $\hat{\Pi}$ and membership matrix Π up to a permutation of community labels under MMDF. The result in Theorem 1 can be simplified by adding some conditions on $\lambda_K(\Pi'\Pi)$ and K , as shown by the following corollary.

Corollary 1 Under $MMDF_n(K, P, \Pi, \rho)$, when conditions of Lemma 2 hold, if we further suppose that $\lambda_K(\Pi'\Pi) = O(\frac{n}{K})$ and $K = O(1)$, with probability at least $1 - o(n^{-3})$, we have

$$\max_{i \in [n]} \|e'_i(\hat{\Pi} - \Pi\mathcal{P})\|_1 = O\left(\frac{1}{\sigma_K(P)}\sqrt{\frac{\gamma \log(n)}{\rho n}}\right).$$

In Corollary 1, the condition $\lambda_K(\Pi'\Pi) = O(\frac{n}{K})$ means that summations of nodes weights in every community are in the same order, and $K = O(1)$ means that network \mathcal{N} has a constant number of communities. The concise form of bound in Corollary 1 is helpful for further analysis. By Mao et al. (2020), we know that $\sigma_K(P)$ is a measure of the separation between communities, and a larger $\sigma_K(P)$ means more well-separated communities. We are interested in the lower bound requirement on $\sigma_K(P)$ to make DFSP's error rate small. By Corollary 1, $\sigma_K(P)$ should shrink slower than $\sqrt{\frac{\gamma \log(n)}{\rho n}}$ for consistent estimation, i.e., $\sigma_K(P) \gg \sqrt{\frac{\gamma \log(n)}{\rho n}}$ should hold to make theoretical bound of error rate in Corollary 1 go to zero as $n \rightarrow +\infty$. Meanwhile, when the network size n is fixed, $\sigma_K(P) \gg \sqrt{\frac{\gamma \log(n)}{n}}$ should hold to make the theoretical upper bound of error rate in Corollary 1 be small with high probability.

For the finiteness of τ in Assumption 1, τ is always finite as long as $A(i, j)$ is a random number generated from MMDF for any distribution \mathcal{F} . The following examples show that γ is finite under different distribution \mathcal{F} as long as Eq (5) holds. Meanwhile, the following examples also provide a more accurate form of Assumption 2 and a more accurate requirement on $\sigma_K(P)$ for a small error rate with high probability when γ has a finite upper bound.

Example 1 When $A(i, j) \sim \text{Normal}(\Omega(i, j), \sigma_A^2)$ for $i, j \in [n]$. When \mathcal{F} is Normal distribution, $\mathbb{E}[A(i, j)] = \Omega(i, j)$ holds by the property of Normal distribution, P can have negative elements

under MMDF, ρ 's range is $(0, +\infty)$ because ρP is not a probability matrix, and $A \in \mathbb{R}^{n \times n}$. For this case, $\gamma = \frac{\sigma_A^2}{\rho}$ is finite. Since γ is in the numerator position of the theoretical upper bound in Corollary 1, increasing σ_A^2 increases DFSP's error rate when $A(i, j) \sim \text{Normal}(\Omega(i, j), \sigma_A^2)$ for $i, j \in [n]$. Setting γ as $\frac{\sigma_A^2}{\rho}$ in ϖ obtains the theoretical upper bound of DFSP's l_1 error, and we see that increasing ρ decreases DFSP's error rate. Note that when \mathcal{F} is Normal distribution and Π is generated from Dirichlet distribution, our MMDF reduces to the multi-way blockmodels for undirected networks proposed in Airoidi et al. (2013). Setting γ as $\frac{\sigma_A^2}{\rho}$, Assumption 2 becomes $\sigma_A^2 n \geq \tau^2 \log(n)$, and it provides a requirement on network size n for theoretical analysis instead of controlling network sparsity, i.e., ρ does not reflect network sparsity because A 's elements can be any finite values for Normal distribution. Finally, setting γ as $\frac{\sigma_A^2}{\rho}$, to make DFSP's error rate small with high probability, $\sigma_K(P) \gg \sqrt{\frac{\sigma_A^2 \log(n)}{\rho^2 n}}$ should hold for fixed n by Corollary 1.

Example 2 When $A(i, j) \sim \text{Binomial}(m, \frac{\Omega(i, j)}{m})$ for any positive integer m for $i, j \in [n]$. When \mathcal{F} is Binomial distribution, $\mathbb{E}[A(i, j)] = \Omega(i, j)$ holds by the property of Binomial distribution, P should have nonnegative elements, ρ 's range is $(0, m]$ because the probability $\frac{\Omega(i, j)}{m} \leq \frac{\rho}{m} \leq 1$, and $A \in \{0, 1, 2, \dots, m\}^{n \times n}$. For this case, $\gamma = \max_{i, j \in [n]} m \frac{\Omega(i, j)}{m} (1 - \frac{\Omega(i, j)}{m}) / \rho \leq \max_{i, j \in [n]} \frac{\Omega(i, j)}{\rho} \leq 1$, i.e., γ is finite. When Ω is fixed, increasing m increases γ , which gives a larger error rate. Setting γ as 1 in ϖ obtains the theoretical upper bound of DFSP's l_1 error and we see that increasing ρ decreases DFSP's error rate. For Binomial distribution, $\tau = m$. Setting $\gamma = 1$ and $\tau = m$, Assumption 2 becomes $\rho n \geq m^2 \log(n)$, so ρ reflects network sparsity and Assumption 2 means a lower bound requirement on network sparsity for Binomial distribution. Finally, setting $\gamma = 1$, to make DFSP's error rate small with high probability, $\sigma_K(P) \gg \sqrt{\frac{\log(n)}{\rho n}}$ should hold for fixed n by Corollary 1.

Example 3 When $A(i, j) \sim \text{Bernoulli}(\Omega(i, j))$ for $i, j \in [n]$ such that MMDF reduces to MMSB. When \mathcal{F} is Bernoulli distribution, $\mathbb{E}[A(i, j)] = \Omega(i, j)$ holds by the property of Bernoulli distribution, P is a nonnegative matrix, ρ 's range is $(0, 1]$ because ρP is a probability matrix, and $A \in \{0, 1\}^{n \times n}$. For Bernoulli distribution, $\text{Var}(A(i, j)) = \Omega(i, j)(1 - \Omega(i, j)) \leq \Omega(i, j) \leq \rho$, which suggests that $\gamma = 1$, a finite number. Sure $\tau = 1$ for this case. Setting $\gamma = 1$ in ϖ obtains the theoretical upper bound of DFSP's l_1 error and we see that increasing ρ decreases DFSP's error rate. Setting $\gamma = 1$ and $\tau = 1$, Assumption 2 becomes $\rho n \geq \log(n)$, so ρ reflects network sparsity and Assumption 2 means a lower bound requirement on network sparsity for Bernoulli distribution. Setting $\gamma = 1$, to make DFSP's error rate small with high probability, $\sigma_K(P) \gg \sqrt{\frac{\log(n)}{\rho n}}$ should hold when n is fixed by Corollary 1. Finally, by the four-step separation condition and sharp threshold criterion introduced in Qing (2022a), our requirement on network sparsity in Assumption 2 and our theoretical bounds in Theorem 1 are theoretically optimal.

Example 4 When $A(i, j) \sim \text{Poisson}(\Omega(i, j))$ for $i, j \in [n]$. By the property of Poisson distribution, $\mathbb{E}[A(i, j)] = \Omega(i, j)$ holds, all entries of P should be nonnegative, ρ 's range is $(0, +\infty)$ because ρP is not a probability matrix for Poisson distribution, and A 's elements are nonnegative integers. For this case, $\gamma = \max_{i, j \in [n]} \frac{\text{Var}(A(i, j))}{\rho} = \max_{i, j \in [n]} \frac{\Omega(i, j)}{\rho} \leq 1$, i.e., γ is finite. Note that the model DCSBM Karrer and Newman (2011) for non-mixed membership networks also lets A 's elements follow the Poisson distribution. For comparison, our MMDF lets A follow the Poisson distribution and allows nodes to have mixed memberships. Setting $\gamma = 1$ in Theorem 1 obtains the theoretical upper bound of DFSP's error rate. Setting $\gamma = 1$, Assumption 2 becomes $\rho n \geq \tau^2 \log(n)$. So, for Poisson distribution, ρ reflects network sparsity and Assumption 2 requires a lower bound on network sparsity for our theoretical guarantee on DFSP's error rate. Finally, setting $\gamma = 1$, DFSP's error rate is small with high probability when $\sigma_K(P) \gg \sqrt{\frac{\log(n)}{\rho n}}$ holds when n is fixed by Corollary 1.

Example 5 When $A(i, j) \sim \text{Laplace}(\Omega(i, j), \sigma_A/\sqrt{2})$ for $i, j \in [n]$. By the property of Laplace distribution, $\mathbb{E}[A(i, j)] = \Omega(i, j)$ holds, all elements of P are real values, ρ 's range is $(0, +\infty)$, $A \in \mathbb{R}^{n \times n}$, and $\text{Var}(A(i, j)) = \sigma_A^2$. Hence, γ is $\frac{\sigma_A^2}{\rho}$, a finite number. Analysis for Assumption 2 and DFSP's error rate when \mathcal{F} is Laplace distribution is similar to that of Example 1, and we omit it here.

Example 6 MMDF can generate signed network by setting $\mathbb{P}(A(i, j) = 1) = \frac{1+\Omega(i, j)}{2}$ and $\mathbb{P}(A(i, j) = -1) = \frac{1-\Omega(i, j)}{2}$. For this case, $\mathbb{E}[A(i, j)] = \Omega(i, j)$ holds, P can have negative entries, ρ 's range is $(0, 1)$ because $-1 \leq \Omega(i, j) \leq 1$, $A \in \{1, -1\}^{n \times n}$, and $\text{Var}(A(i, j)) = 1 - \Omega^2(i, j) \leq 1$, i.e., $\gamma \leq \frac{1}{\rho}$ is finite. τ 's upper bound is 2 for this case. Setting γ as $\frac{1}{\rho}$ in Theorem 1 obtains the theoretical upper bound of DFSP's error rate and we see that increasing ρ decreases the error rate. Setting $\gamma = \frac{1}{\rho}$ and $\tau = 2$, Assumption 2 becomes $n \geq 4\log(n)$, and it means a lower bound requirement on network size n similar to the cases when \mathcal{F} is Normal and Laplace distributions. So, ρ does not mean network sparsity for a signed network. Finally, setting $\gamma = \frac{1}{\rho}$, DFSP's error rate is small with high probability when $\sigma_K(P) \gg \sqrt{\frac{\log(n)}{\rho^2 n}}$ holds when n is fixed by Corollary 1.

More than the above six distributions, the distribution-free property of MMDF allows \mathcal{F} to be other distributions as long as Eq (5) holds. For example, \mathcal{F} can be Double exponential, Exponential, Gamma, Laplace, and Uniform distributions in <http://www.stat.rice.edu/~dobelman/courses/texts/distributions>. Details on probability mass function or probability density function on distributions discussed in this paper can also be found in the above URL link. Generally speaking, the distribution-free property guarantees the generality of our model, our DFSP algorithm as well as our theoretical results.

We further consider a weighted network generated from MMDF when P is set as $P = \beta I_K + (1 - \beta)\mathbf{1}\mathbf{1}'$ for $\beta \in (0, 1]$ (note that $\sigma_K(P) = \beta$), $\lambda_K(\Pi'\Pi) = O(\frac{\rho}{K})$ and $K = O(1)$. Since $\Omega = \Pi\rho\Pi' = \Pi'\tilde{P}\Pi'$, where we set $\tilde{P} = \rho P$. Set $p_{\text{in}} = \rho, p_{\text{out}} = \rho(1 - \beta)$ (note that $p_{\text{in}} = \max_{k, l \in [K]} \tilde{P}(k, l)$, and $p_{\text{out}} = \min_{k, l \in [K]} \tilde{P}(k, l)$). By Corollary 1, the upper bound of error rate is $O(\frac{1}{\beta} \sqrt{\frac{\gamma \log(n)}{\rho n}})$, which suggests that increasing β decreases error rate. Meanwhile, to obtain consistent estimation, $\frac{p_{\text{in}} - p_{\text{out}}}{\sqrt{p_{\text{in}}}} = \beta\sqrt{\rho}$ should shrink slower than $\sqrt{\frac{\gamma \log(n)}{n}}$, and this threshold holds for any distribution \mathcal{F} under MMDF as long as Eq (5) holds. Especially, when \mathcal{F} is Bernoulli distribution and all nodes are pure such that MMDF reduces to SBM, the above threshold is the classical separation condition in Corollary 1 of McSherry (2001) since γ is 1 for Bernoulli distribution, and this also guarantees the optimality of our theoretical results.

5. Simulations

In this section, we study DFSP's performance over a series of simulations when A is generated under MMDF for different distribution \mathcal{F} . Since MMDF is the first model for a mixed membership weighted network in which A 's elements can be generated from any distribution \mathcal{F} as long as Equation (5) holds, and DFSP can consistently estimate memberships under MMDF, there are no comparison algorithms of DFSP for numerical studies. We measure the performance of DFSP by the following error rate:

$$\min_{\mathcal{P} \in \{K \times K \text{ permutation matrix}\}} \frac{1}{n} \|\hat{\Pi} - \Pi\mathcal{P}\|_1.$$

For all simulations, unless specified, set $n = 200, K = 3$, and $n_0 = 40$, where n_0 denotes the number of pure nodes for each community. Let all mixed nodes have four different memberships $(0.4, 0.4, 0.2), (0.4, 0.2, 0.4), (0.2, 0.4, 0.4)$ and $(1/3, 1/3, 1/3)$, each with $\frac{n-3n_0}{4}$ number of nodes. The connectivity matrix P and sparsity parameter ρ are set independently for each experiment. Note that maximum entries of ρP are allowed to be larger than 1 under MMDF when \mathcal{F} is not Bernoulli

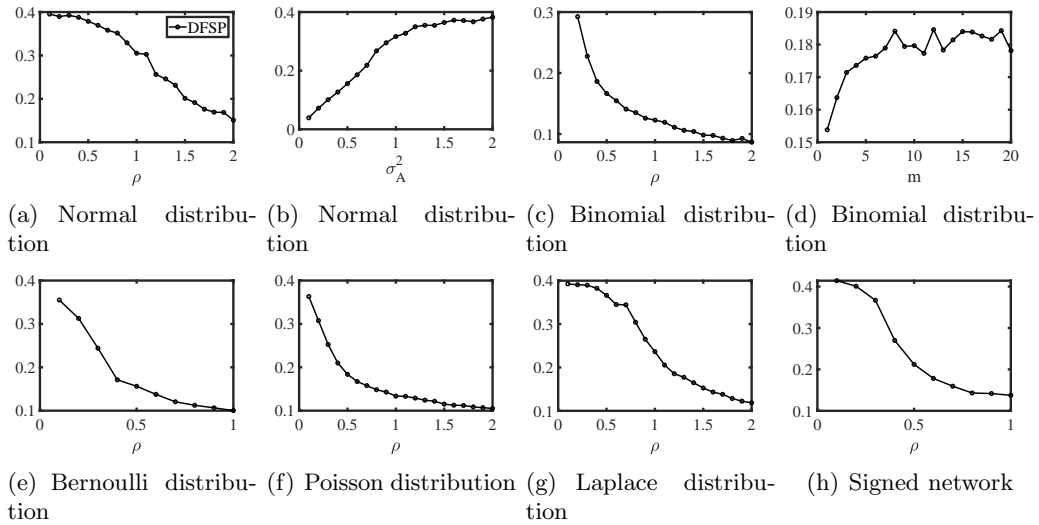


Figure 2: Numerical results of Experiments 1-6. y-axis: error rate.

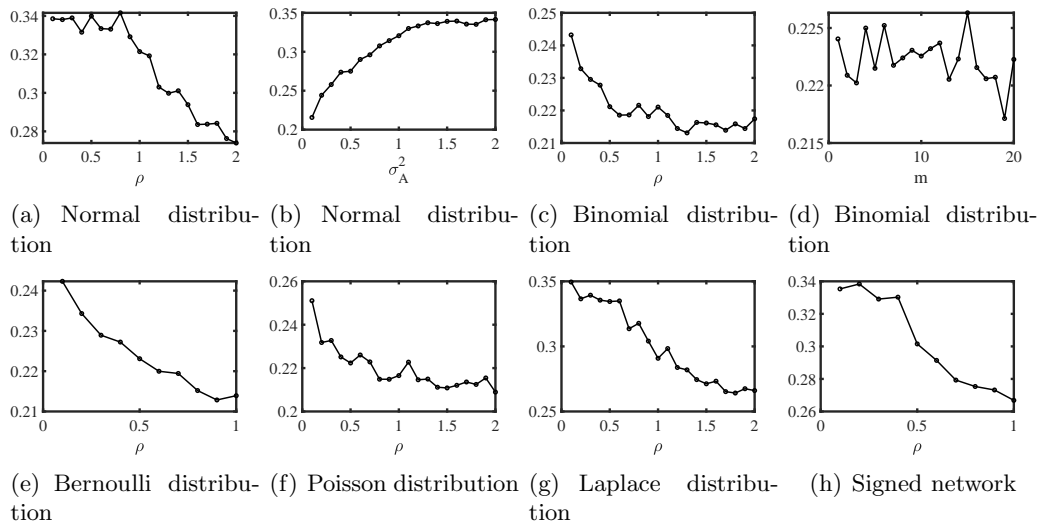


Figure 3: Numerical results of Experiments 1-6 without pure nodes: the six panels are plotted under the same settings as panels (a)-(h) of Figure 2 except that $n_0 = 0$ (i.e., no pure node for each community), a case for DFSP's sensitivity on MMDF's pure nodes condition. Compared with error rates in Figure 2, though DFSP performs slightly poorer, it still can estimate memberships even when there are no pure nodes which suggests that DFSP is not sensitive to MMDF's pure nodes condition. y-axis: error rate.

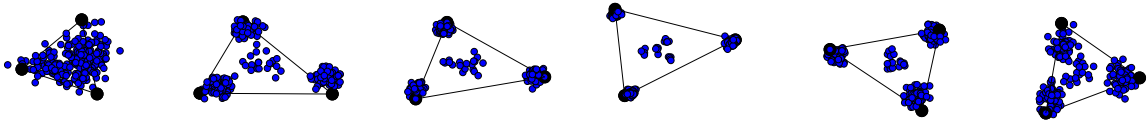
distribution because entries of ρP are not probabilities when F is not Bernoulli. Meanwhile, in all numerical studies, the only criteria for choosing P is, P should obey Equation (4), and P 's entries should be positive or negative relying on \mathcal{F} . Each simulation experiment contains the following steps:

(a) Set $\Omega = \rho \Pi P \Pi'$.

(b) Let $A(i, j)$ be a random number generated from distribution \mathcal{F} with expectation $\Omega(i, j)$ for $1 \leq i < j \leq n$, set $A(j, i) = A(i, j)$ to make A be symmetric, and let A 's diagonal elements be zero since we do not consider self-edges.

(c) Apply DFSP to A with K communities. Record error rate.

(d) Repeat (b)-(c) 50 times, and report the averaged error rates over the 50 repetitions.



(a) $\rho = 1, \sigma_A^2 = 2$. (b) $\rho = 3, \sigma_A^2 = 2$. (c) $\rho = 5, \sigma_A^2 = 2$. (d) $\rho = 1, \sigma_A^2 = \frac{1}{5}$. (e) $\rho = 1, \sigma_A^2 = \frac{3}{5}$. (f) $\rho = 1, \sigma_A^2 = 1$.

Figure 4: Normal distribution: \hat{U} . Each point is a row of \hat{U} , and the three black points represent the three rows of $\hat{U}(\hat{\mathcal{L}}, :)$, where $\hat{\mathcal{L}}$ is estimated index set returned by SP. Since $K = 3$, for visualization, we have projected and rotated these points from \mathbb{R}^3 to \mathbb{R}^2 .

Experiment 1: Normal distribution. Set \mathcal{F} as Normal distribution such that $A(i, j) \sim \text{Normal}(\Omega(i, j), \sigma_A^2)$ for some σ_A^2 . Set P as

$$P = \begin{bmatrix} -1 & -0.2 & 0.3 \\ -0.2 & 0.9 & 0.3 \\ 0.3 & 0.3 & 0.9 \end{bmatrix}.$$

Note that when \mathcal{F} is Normal distribution, P is allowed to have negative entries and A can have negative elements under MMDF. This experiment has two sub-experiments.

Experiment 1[a]. Let $\sigma_A^2 = 2$, and ρ range in $\{0.1, 0.2, \dots, 2\}$. The results are presented in Panel (a) of Figure 2. We see that DFSP performs better as ρ increases, and this is consistent with our Corollary 1. Meanwhile, we also plot \hat{U} in Panels (a), (b), and (c) of Figure 4 for different ρ when σ_A^2 is fixed, where we see the estimated simplex obtained from \hat{U} when applying SP algorithm is more “close” to the Ideal Simplex in Figure 1 when increasing ρ , and this explains why DFSP performs better when ρ increases.

Experiment 1[b]. Let $\rho = 0.5$, and σ_A^2 range in $\{0.1, 0.2, \dots, 2\}$. The results are presented in Panel (b) of Figure 2, and we find that DFSP performs poorer as σ_A^2 increases which match the analysis in Example 1. Panels (d), (e), and (f) of Figure 4 show plots of \hat{U} for different σ_A^2 when ρ is fixed, and the three panels show that the estimated simplex obtained from \hat{U} is more “farther” to the Ideal Simplex in Figure 1 when increasing σ_A^2 , and this explains why DFSP performs poorer when σ_A^2 increases.

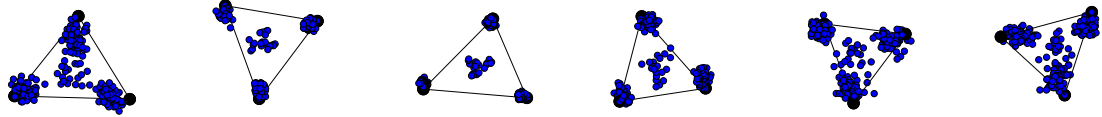
Experiment 2: Binomial distribution. Set \mathcal{F} as Binomial distribution such that $A(i, j) \sim \text{Binomial}(m, \frac{\Omega(i, j)}{m})$ for some positive integer m . Note that, since $\Omega(i, j) \leq \rho$ and $\frac{\Omega(i, j)}{m}$ is probability for all nodes, ρ should be set smaller than m in this experiment. Meanwhile, when \mathcal{F} is Binomial, elements of A take values from $\{0, 1, 2, \dots, m\}$. Set P as

$$P = \begin{bmatrix} 1 & 0.2 & 0.3 \\ 0.2 & 0.9 & 0.3 \\ 0.3 & 0.3 & 0.9 \end{bmatrix}.$$

This experiment has two sub-experiments.

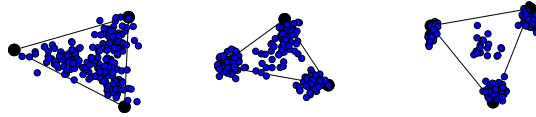
Experiment 2[a]. Let $m = 4$, and ρ range in $\{0.1, 0.2, \dots, 2\}$. Results are shown in Panel (c) of Figure 2, and we see that DFSP enjoys better performance as ρ increases when \mathcal{F} is Binomial distribution. Meanwhile, panels (a), (b), and (c) of Figure 5 show plots of \hat{U} when changing ρ . We see that a more clear structure of simplex appears as ρ increases, thus an easier case for DFSP to recover node memberships.

Experiment 2[b]. Let $\rho = 0.5$, and m range in $\{1, 2, \dots, 20\}$. Panel (d) of Figure 2 displays the results. It suggests that increasing m increases the error rate of DFSP, and this is consistent with the theoretical findings in Example 2. Meanwhile, we also plot \hat{U} for different m when ρ is fixed in Figure 5. We see that the estimated simplex obtained from \hat{U} via applying the SP algorithm is farther to the Ideal Simplex when m increases, creating a harder case for DFSP to recover Π .



(a) $\rho = 1, m = 5$. (b) $\rho = 3, m = 5$. (c) $\rho = 5, m = 5$. (d) $\rho = 1, m = 1$. (e) $\rho = 1, m = 3$. (f) $\rho = 1, m = 6$.

Figure 5: Binomial distribution: \hat{U} .



(a) $\rho = 0.2$. (b) $\rho = 0.6$. (c) $\rho = 1$.

Figure 6: Bernoulli distribution: \hat{U} .

Experiment 3: Bernoulli distribution. Set \mathcal{F} as Bernoulli distribution such that $A(i, j) \sim \text{Bernoulli}(\Omega(i, j))$. Set P the same as Experiment 2. Meanwhile, for the Bernoulli case, all entries of A are either 0 or 1. Let ρ range in $\{0.1, 0.2, \dots, 1\}$. Panel (e) of Figure 2 shows the results. Similarly, we can plot \hat{U} for this Experiment 3 (also for Experiments 4, 5, and 6) by changing ρ as Experiments 1 and 2, and Figure 6 displays plots of \hat{U} .

Experiment 4: Poisson distribution. Set \mathcal{F} as Poisson distribution such that $A(i, j) \sim \text{Poisson}(\Omega(i, j))$. Set P the same as Experiment 2. For Poisson distribution, all entries of A take values from $\{0, 1, 2, \dots\}$. Let ρ range in $\{0.1, 0.2, \dots, 2\}$. Panel (f) of Figure 2 displays the results.

Experiment 5: Laplace distribution. Set \mathcal{F} as Laplace distribution such that $A(i, j) \sim \text{Laplace}(\Omega(i, j), \sigma_A/\sqrt{2})$. Set $\sigma_A = 1$, and P same as Experiment 1. Let ρ range in $\{0.1, 0.2, \dots, 2\}$. Panel (g) of Figure 2 displays the results.

Experiment 6: Signed network. For signed network when $\mathbb{P}(A(i, j) = 1) = \frac{1+\Omega(i, j)}{2}$ and $\mathbb{P}(A(i, j) = -1) = \frac{1-\Omega(i, j)}{2}$, let $n = 300$, each community own $n_0 = 80$ number of pure nodes, all mixed nodes's memberships and P be the same as that of Experiment 1. Let ρ range in $\{0.1, 0.2, \dots, 1\}$. Panel (h) of Figure 2 displays the results.

Experiment 7: Changing β . Let $\beta \in \{0.1, 0.2, \dots, 1\}$. Set $\rho = 1$, and P as

$$P = \begin{bmatrix} 1 & 1 - \beta & 1 - \beta \\ 1 - \beta & 1 & 1 - \beta \\ 1 - \beta & 1 - \beta & 1 \end{bmatrix}.$$

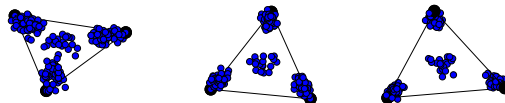
Since $\sigma_K(P) = \beta$, increasing β decreases error rate by the analysis given after Example 6. This experiment has six sub-experiments.

Experiment 7[a]. Let \mathcal{F} be Normal distribution such that $A(i, j) \sim \text{Normal}(\Omega(i, j), 2)$.

Experiment 7[b]. Let \mathcal{F} be Binomial distribution such that $A(i, j) \sim \text{Binomial}(4, \frac{\Omega(i, j)}{4})$.

Experiment 7[c]. Let \mathcal{F} be Bernoulli distribution such that $A(i, j) \sim \text{Bernoulli}(\Omega(i, j))$.

Experiment 7[d]. Let \mathcal{F} be Poisson distribution such that $A(i, j) \sim \text{Poisson}(\Omega(i, j))$.



(a) $\rho = 1$. (b) $\rho = 3$. (c) $\rho = 5$.

Figure 7: Poisson distribution: \hat{U} .

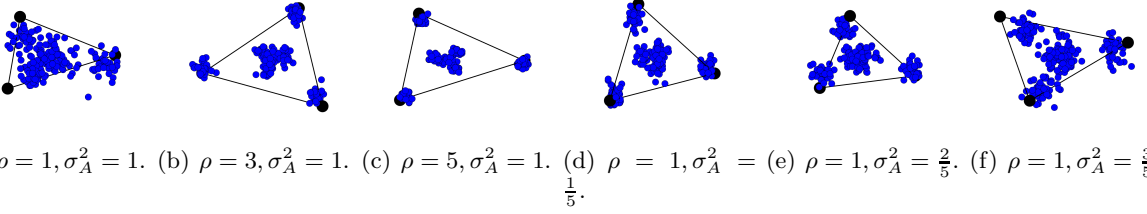


Figure 8: Laplace distribution: \hat{U} .

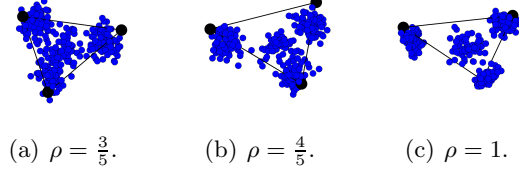


Figure 9: Signed network: \hat{U} .

Experiment 7[e]. Let \mathcal{F} be Laplace distribution such that $A(i, j) \sim \text{Laplace}(\Omega(i, j), 1)$.

Experiment 7[f]. Let \mathcal{F} be distribution of signed network such that $\mathbb{P}(A(i, j) = 1) = \frac{1+\Omega(i, j)}{2}$ and $\mathbb{P}(A(i, j) = -1) = \frac{1-\Omega(i, j)}{2}$.

The results of Experiment 7 are displayed in Figure 10. It suggests that DFSP performs better when β increases, and this supports our theoretical findings.

Remark 2 For visuality, we plot A generated under MMDF for different \mathcal{F} in this remark. We let $K = 2$, each community have n_0 pure nodes, each mixed nodes have membership $(0.5, 0.5)$, and P be

$$P_a = \begin{bmatrix} 1 & 0.1 \\ 0.1 & 0.9 \end{bmatrix} \text{ or } P_b = \begin{bmatrix} 1 & -0.1 \\ -0.1 & -0.9 \end{bmatrix}.$$

Model set-up 1: When $A(i, j) \sim \text{Normal}(\Omega(i, j), \sigma_A^2)$, set $n = 15, n_0 = 6, \sigma_A^2 = 1, \rho = 8$ and P as P_b . Panel (a) of Figure 11 shows an adjacency matrix A generated under MMDF for model set-up 1, where we also report DFSP's error rate. With given A and known memberships Π for this set-up, readers can apply DFSP to A to check its effectiveness.

Model set-up 2: When $A(i, j) \sim \text{Binomial}(m, \Omega(i, j)/m)$, set $n = 26, n_0 = 11, \rho = 3, m = 7$, and P as P_a . Panel (b) of Figure 11 shows an adjacency matrix A generated under MMDF for this set-up.

Model set-up 3: When $A(i, j) \sim \text{Bernoulli}(\Omega(i, j))$, set $n = 32, n_0 = 14, \rho = 0.9$ and P as P_a . Panel (c) of Figure 11 shows an adjacency matrix A generated under MMDF for this set-up.

Model set-up 4: When $A(i, j) \sim \text{Poisson}(\Omega(i, j))$, set $n = 20, n_0 = 8, \rho = 40$ and P as P_a . Panel (d) of Figure 11 shows an adjacency matrix A generated under MMDF for this set-up.

Model set-up 5: When $A(i, j) \sim \text{Laplace}(\Omega(i, j), \sigma_A/2)$, set $n = 16, n_0 = 7, \sigma = 1, \rho = 9$ and P as P_b . Panel (e) of Figure 11 shows an adjacency matrix A generated under MMDF for this set-up.

Model set-up 6: For signed network when $\mathbb{P}(A(i, j) = 1) = \frac{1+\Omega(i, j)}{2}$ and $\mathbb{P}(A(i, j) = -1) = \frac{1-\Omega(i, j)}{2}$, set $n = 32, n_0 = 15, \rho = 0.9$ and P as P_b . Panel (f) of Figure 11 shows an adjacency matrix A generated under MMDF for this set-up.

6. Application to real-world weighted networks

Recall that the $K \times 1$ vector $\hat{\Pi}(i, :)$ is the estimated membership for node $i \in [n]$, we need the following definition.

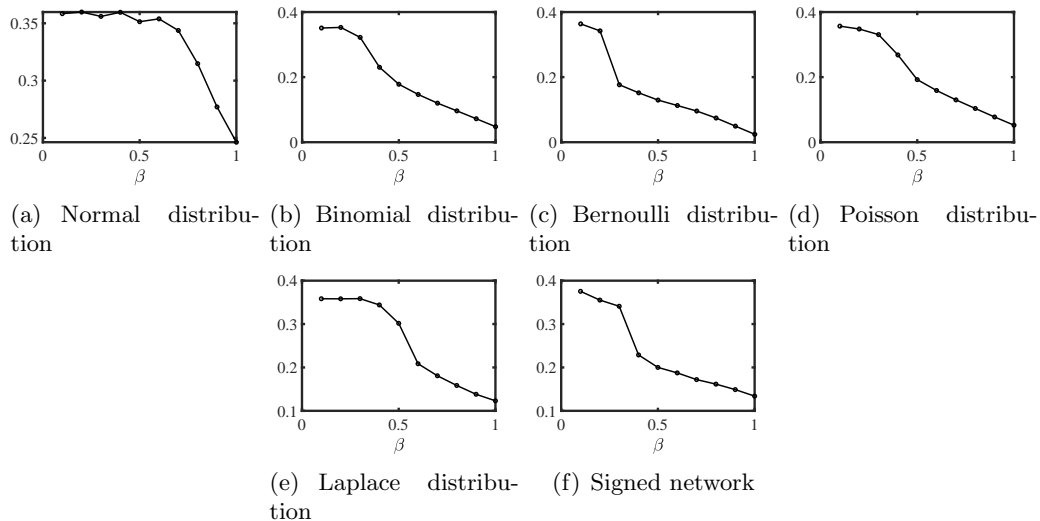


Figure 10: Numerical results of Experiment 7. y-axis: error rate.

Definition 2 For a constant $\zeta \in [0.6, 1)$, let $\varphi(\zeta) = \frac{|\{i \in [n]: \hat{\Pi}_{i, \max} \geq \zeta\}|}{n}$, where $\hat{\Pi}_{i, \max} = \max_{1 \leq k \leq K} \hat{\Pi}(i, k)$. Call $\varphi(\zeta)$ the network purity, ζ the purity threshold, and $\hat{\Pi}_{i, \max}$ the purity of node i .

In the definition of purity, node i is regarded as a highly pure node if $\hat{\Pi}_{i, \max} \geq \zeta$, thus $\varphi(\zeta)$ represents the proportion of highly pure nodes and it is useful in investigating the purity of real-world weighted networks. Sure, increasing ζ increases the requirement for network purity.

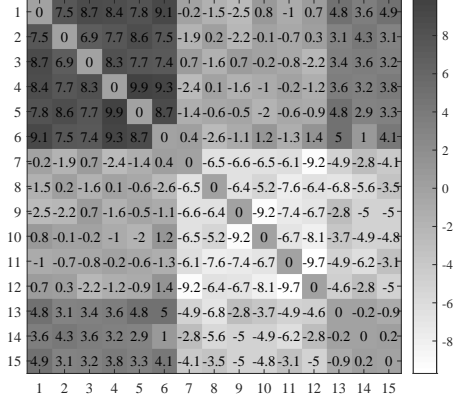
We apply DFSP to five real-world weighted networks, Gahuku-Gama subtribes Read (1954), Karate-club-weighted Zachary (1977), Coauthorships in network science (Coauthorships for short) Newman (2006), Condensed matter collaborations 1999 (Con-mat-1999 for short) Newman (2001), and Condensed matter collaborations 2003 (Con-mat-2003 for short) Newman (2001). For visualization, Figure 12 shows adjacency matrices of the first two weighted networks, and we see that all edge weights for the Karate-club-weighted network are nonnegative and Gahuku-Gama subtribes is a signed network. For the other three networks, all edge weights are nonnegative. Table 2 summarizes basic information for these networks. A brief introduction to these networks is given below.

Table 2: Five real-world weighted networks.

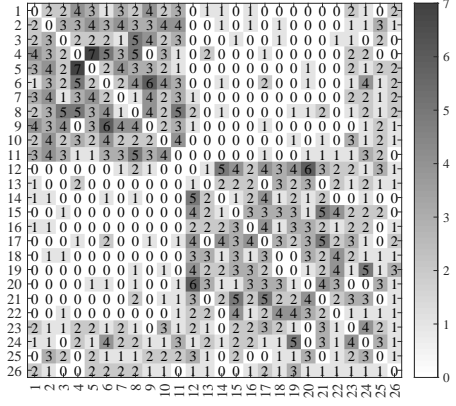
	n	K	$\max_{i,j} A(i, j)$	$\min_{i,j} A(i, j)$	#Edges	%Positive edges
Gahuku-Gama subtribes	16	3	1	-1	58	50%
Karate-club-weighted	34	2	7	0	78	100%
Coauthorships	379	Unknown	4.75	0	914	100%
Con-mat-1999	13861	Unknown	22.3333	0	44619	100%
Con-mat-2003	27519	Unknown	35.2	0	116181	100%

Gahuku-Gama subtribes: This data is the signed social network of tribes of the Gahuku-Gama alliance structure of the Eastern Central Highlands of New Guinea Kunegis (2013). A positive link means alliance while a negative link means enmity. Meanwhile, this network has 3 communities, its node labels shown in Figure 9 (b) from Yang et al. (2007) are regarded as ground truth here. This data can be downloaded from <http://konect.cc/networks/ucidata-gama/>.

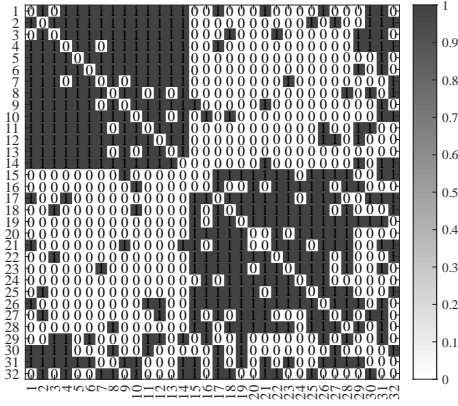
Karate-club-weighted: In this network, node means member of a karate club in a university, and edge denotes the relative strength of associations. This network is the weighted version of the classical Karate club network. So, the number of communities is 2 and true labels for all members are known for Karate-weighted. This data can be downloaded from <http://vlado.fmf.uni-lj.si/pub/networks> and the classical Karate club network and its true labels can be found in <http://www-personal.umich.edu/~me>



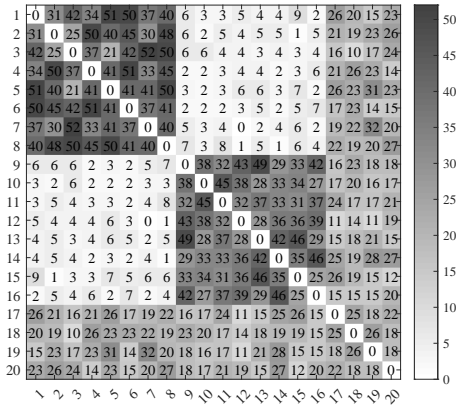
(a) A of model set-up 1



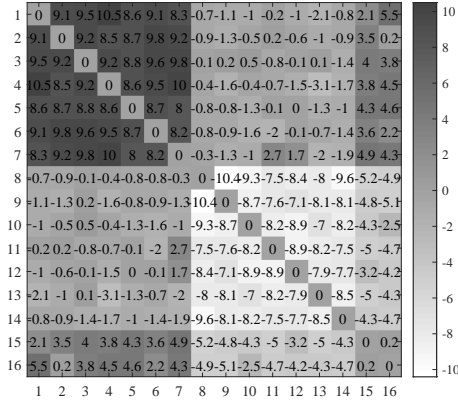
(b) A of model set-up 2



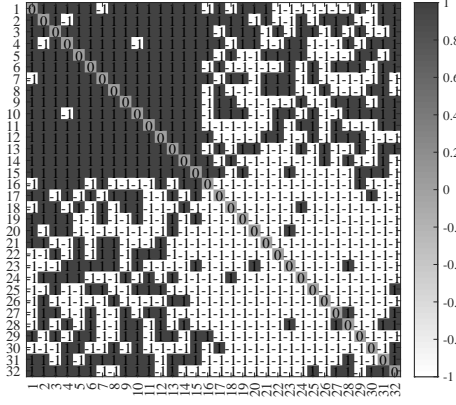
(c) A of model set-up 3



(d) A of model set-up 4

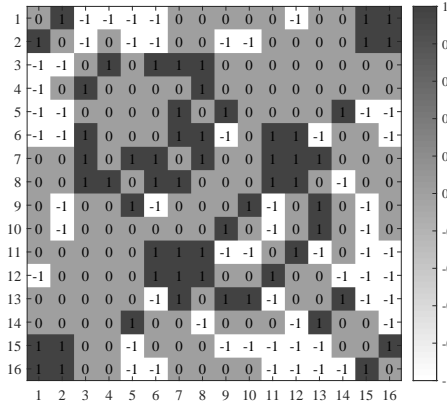


(e) A of model set-up 5

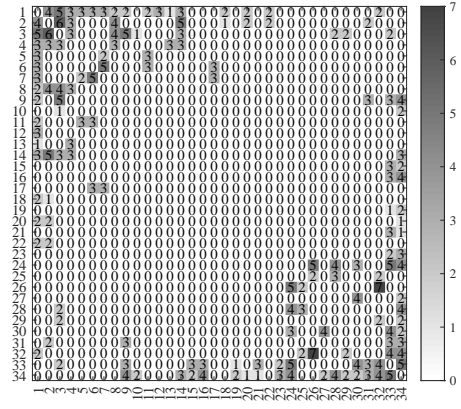


(f) A of model set-up 6

Figure 11: Illustration for weighted networks' adjacency matrices generated under MMDF. For A in panel (a)-(f), DFSP's error rate are 0.0031, 0.0136, 0.0264, 0.0064, 0.0066, and 0.0390, respectively. In panels (a) and (e), we keep A 's entries in one decimal for visualization beauty.



(a) Gahuku-Gama subtribes



(b) Karate-club-weighted

Figure 12: Adjacency matrices of Gahuku-Gama subtribes and Karate-club-weighted.

Coauthorships: This data can be downloaded from <http://www-personal.umich.edu/~mejn/netdata/>. In this network, node denotes scientist, and weights provided by the original papers mean coauthorship. The original network has 1589 nodes, and only 379 nodes fall in the largest connected component, and we focus on the giant component in this paper. To find K , we plot the leading 20 singular values of its adjacency matrix. Results shown in Figure 13 suggest that K is 2.

Con-mat-1999: This data can be downloaded from <http://www-personal.umich.edu/~mejn/netdata/>. It is a weighted network of coauthorships between scientists posting preprints on the Condensed Matter E-Print Archive between Jan 1, 1995 and December 31, 1999. Edge weights are provided by the original papers. The original network has 16726 nodes, and its largest connected component which we study in this paper has 13861 nodes. Eigen-gap shown in Figure 13 suggests that K is 2 for this network.

Con-mat-2003: It is updated network of Con-mat-1999. This network has 31163 nodes, and the largest connected component used in this paper has 27519 nodes. Eigen-gap shown in Figure 13 also suggests that K is 2 for Con-mat-2003.

Let $\hat{\Pi}$ be the estimated membership matrix returned by applying DFSP on Gahuku-Gama subtribes network with 3 communities, and set $\hat{c}_i = \arg \max_{1 \leq k \leq K} \hat{\Pi}(i, k)$ for $1 \leq i \leq n$ as the estimated label for node i . By comparing \hat{c} with the true labels for the Gahuku-Gama subtribes network, we find that DFSP misclusters 0 nodes out of 16. Similarly, applying DFSP on the Karate-club-weighted network with 2 communities obtains estimated labels for all nodes, and we find that DFSP misclusters 0 nodes out of 34.

Since the true membership matrix is unknown for the Coauthorships network, we apply DFSP to this data with two clusters to obtain the estimated membership matrix $\hat{\Pi}$, and then compute network purity for different choices of the purity threshold ζ based on $\hat{\Pi}$. Applying DFSP to Coauthorships with two clusters to estimate the membership matrix takes around 0.01 seconds. The true membership matrix is also unknown for the Con-mat-1999 (and Con-mat-2003) network, and we also compute its purity. Applying DFSP to Con-mat-1999 (and Con-mat-2003) with two clusters to estimate the membership matrix takes around 9.5 seconds (40 seconds). Meanwhile, for comparison, we provide purity of Gahuku-Gama subtribes and Karate-club-weighted networks. The results are displayed in Table 3. We see that (1) $\phi(0.9)$ for Gahuku-Gama subtribes is 0.8750, which is quite small compared with 1, thus this network has $16 - 16\phi(0.9) = 2$ highly mixed nodes for a large purity threshold 0.9. (2) for Karate-club weighted network, it has $34 - 34\phi(0.85) \approx 4$ highly mixed nodes for purity threshold 0.85, $34 - 34\phi(0.9) \approx 7$ highly mixed nodes for a large purity threshold 0.9. The purity of the Karate-club-weighted network is smaller than that of the Gahuku-Gama subtribes network for the same purity threshold ζ , thus Karate-club-weighted is more mixed than Gahuku-Gama subtribes. (3) for Coauthorships network, it has $379 - 379\phi(0.85) \approx 9$

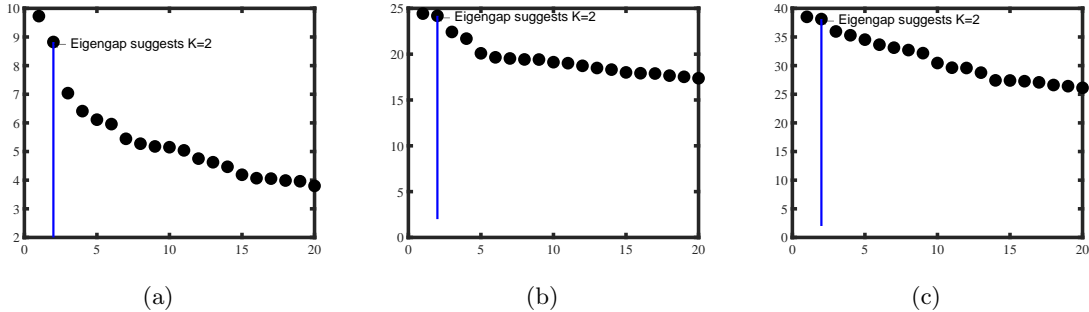


Figure 13: Panels (a),(b) and (c) show leading 20 singular values of adjacency matrices for Coauthorships, Cond-mat-1999 and Cond-mat-2003, respectively.

highly mixed nodes when $\zeta = 0.85$, and $379 - 379\phi(0.9) \approx 23$ highly mixed nodes when $\zeta = 0.9$. Compared with Gahuku-Gama subtribes and Karate-club-weighted, we see that Coauthorships is a highly pure network since its purity is always larger than Gahuku-Gama subtribes and Karate-club-weighted for the same purity threshold. (4) for Con-mat-1999, it has $13861 - 13861\phi(0.7) = 2039$ highly mixed nodes for a small purity threshold 0.7. Con-mat-1999 is a highly mixed network since its purity is always smaller than that of Gahuku-Gama subtribes, Karate-club-weighted, and Coauthorships for the same purity threshold. Similar arguments hold for Con-mat-2003, and we find that Con-mat-2003 is more mixed than the other four networks. For visibility, Figure 14 depicts communities returned by DFSP for Gahuku-Gama subtribes, Karate-club-weighted, and Coauthorships networks, where we also highlight highly mixed nodes detected by DFSP.

Table 3: Purity for the five network data sets in Table 2 when varying threshold ζ .

	Gahuku-Gama subtribes	Karate-club-weighted	Coauthorships	Con-mat-1999	Con-mat-2003
$\varphi(0.7)$	0.9375	0.9412	0.9868	0.8529	0.7780
$\varphi(0.75)$	0.9375	0.9118	0.9868	0.8003	0.7034
$\varphi(0.8)$	0.9375	0.8824	0.9789	0.7404	0.6336
$\varphi(0.85)$	0.9375	0.8824	0.9763	0.6723	0.5502
$\varphi(0.9)$	0.8750	0.7941	0.9393	0.5777	0.4470

7. Conclusion

In this article, we introduce a general, flexible and identifiable mixed membership distribution-free model, which is, to the best of our knowledge, the first model for mixed membership weighted network in which edges can be generated from arbitrary distribution as long as Equation (5) holds, where Equation (5) is directly related with the latent community information. The distribution-free property of the proposed model even allows elements of the adjacency matrix to be any finite real value. The model provides exploratory tools for studying latent structural information of networks in which nodes belong to multiple communities and edge weights can be generated from any distribution. An efficient spectral algorithm designed based on the simplex structure inherent in the eigenvectors of the population adjacency matrix is applied to fit the model. We show the estimation consistency of the algorithm under our model by considering network sparsity and taking the advantage of recent technique on row-wise eigenvectors deviation. Our theoretic framework on consistent estimation also enjoys distribution-free property such that results, when edge weights follow different distributions, can be obtained immediately. Separation conditions for weighted networks generated from different distributions under MMDF are obtained. Numerical results obtained by applying the algorithm to detect community membership of various simulated mixed membership weighted networks when edge weights are generated from different distributions under

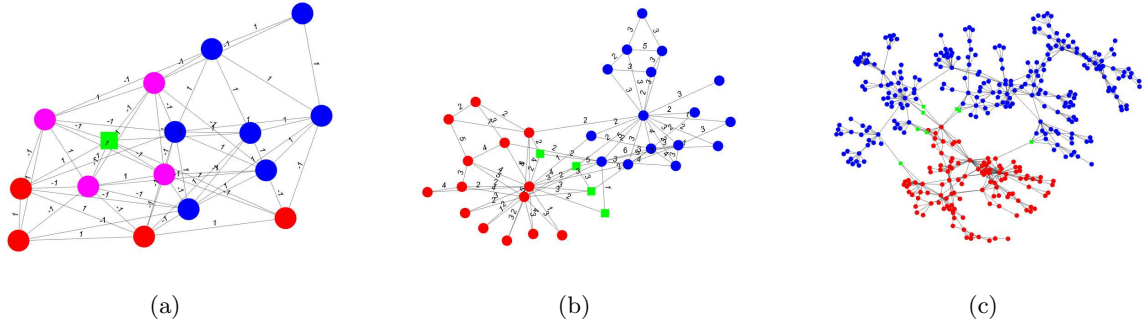


Figure 14: Panels (a)-(c): communities detected by DFSP for Gahuku-Gama subtribes, Karate-club-weighted, and Coauthorships networks. Colors indicate communities and the green square indicates highly mixed nodes, where communities are obtained by \hat{c} and we call node i highly mixed node if $\hat{\Pi}_{i,\max} \leq 0.8$. For visualization, we do not show edge weights for Coauthorships.

the model are consistent with the theoretical results. Numerical results on real-world social weighted networks reveal the difference in network purity. MMDF is a generative model without constraint on a specific distribution. We expect that the mixed membership distribution-free model and the algorithm fitting the model proposed in this article will have wide applications in learning and understanding the latent structure of mixed membership weighted networks in network science, just as the famous mixed membership stochastic blockmodels has been widely studied in recent years.

Acknowledgements

This research was funded by the High-level personal project of Jiangsu Province NO.JSSCBS20211218.

References

- Emmanuel Abbe. Community detection and stochastic block models: recent developments. *The Journal of Machine Learning Research*, 18(1):6446–6531, 2017.
- Emmanuel Abbe and Colin Sandon. Community detection in general stochastic block models: Fundamental limits and efficient algorithms for recovery. In *2015 IEEE 56th Annual Symposium on Foundations of Computer Science*, pages 670–688, 2015.
- Emmanuel Abbe, Afonso S. Bandeira, and Georgina Hall. Exact recovery in the stochastic block model. *IEEE Transactions on Information Theory*, 62(1):471–487, 2016.
- Christopher Aicher, Abigail Z. Jacobs, and Aaron Clauset. Learning latent block structure in weighted networks. *Journal of Complex Networks*, 3(2):221–248, 2015.
- Edoardo M. Airoldi, David M. Blei, Stephen E. Fienberg, and Eric P. Xing. Mixed membership stochastic blockmodels. *Journal of Machine Learning Research*, 9:1981–2014, 2008.
- Edoardo M. Airoldi, Xiaopei Wang, and Xiaodong Lin. Multi-way blockmodels for analyzing coordinated high-dimensional responses. *The Annals of Applied Statistics*, 7(4):2431–2457, 2013.
- Joshua Cape, Minh Tang, and Carey E. Priebe. The two-to-infinity norm and singular subspace geometry with applications to high-dimensional statistics. *Annals of Statistics*, 47(5):2405–2439, 2019.

- Yudong Chen, Xiaodong Li, and Jiaming Xu. Convexified modularity maximization for degree-corrected stochastic block models. *Annals of Statistics*, 46(4):1573–1602, 2018.
- Yuxin Chen, Yuejie Chi, Jianqing Fan, and Cong Ma. Spectral methods for data science: A statistical perspective. *Foundations and Trends® in Machine Learning*, 14(5):566–806, 2021.
- David S. Choi, Patrick J. Wolfe, and Edoardo M. Airoidi. Stochastic blockmodels with a growing number of classes. *Biometrika*, 99(2):273–284, 2011.
- Adrien Dulac, Eric Gaussier, and Christine Largeton. Mixed-membership stochastic block models for weighted networks. In *Conference on Uncertainty in Artificial Intelligence (UAI)*, volume 124, pages 679–688, 2020.
- Santo Fortunato. Community detection in graphs. *Physics reports*, 486(3-5):75–174, 2010.
- Santo Fortunato and Darko Hric. Community detection in networks: A user guide. *Physics reports*, 659:1–44, 2016.
- Chao Gao, Zongming Ma, Anderson Y. Zhang, and Harrison H. Zhou. Achieving optimal misclassification proportion in stochastic block models. *Journal of Machine Learning Research*, 18(60):1–45, 2017.
- Nicolas Gillis and Stephen A. Vavasis. Semidefinite programming based preconditioning for more robust near-separable nonnegative matrix factorization. *SIAM Journal on Optimization*, 25(1):677–698, 2015.
- Bruce Hajek, Yihong Wu, and Jiaming Xu. Achieving exact cluster recovery threshold via semidefinite programming. *IEEE Transactions on Information Theory*, 62(5):2788–2797, 2016.
- Paul W. Holland, Kathryn Blackmond Laskey, and Samuel Leinhardt. Stochastic blockmodels: First steps. *Social Networks*, 5(2):109–137, 1983.
- Jiashun Jin. Fast community detection by SCORE. *Annals of Statistics*, 43(1):57–89, 2015.
- Jiashun Jin, Zheng Tracy Ke, and Shengming Luo. Estimating network memberships by simplex vertex hunting. *arXiv: Methodology*, 2017.
- Varun Jog and Po-Ling Loh. Information-theoretic bounds for exact recovery in weighted stochastic block models using the renyi divergence. *arXiv preprint arXiv:1509.06418*, 2015.
- Antony Joseph and Bin Yu. Impact of regularization on spectral clustering. *Annals of Statistics*, 44(4):1765–1791, 2016.
- Brian Karrer and M. E. J. Newman. Stochastic blockmodels and community structure in networks. *Physical Review E*, 83(1):16107, 2011.
- Jérôme Kunegis. Konect: the koblenz network collection. In *Proceedings of the 22nd international conference on world wide web*, pages 1343–1350, 2013.
- Pierre Latouche, Etienne Birmelé, and Christophe Ambroise. Overlapping stochastic block models with application to the french political blogosphere. *Annals of Applied Statistics*, 5(1):309–336, 2011.
- Jing Lei and Alessandro Rinaldo. Consistency of spectral clustering in stochastic block models. *Annals of Statistics*, 43(1):215–237, 2015.
- Xueyu Mao, Purnamrita Sarkar, and Deepayan Chakrabarti. Overlapping clustering models, and one (class) svm to bind them all. In *Advances in Neural Information Processing Systems*, volume 31, pages 2126–2136, 2018.

- Xueyu Mao, Purnamrita Sarkar, and Deepayan Chakrabarti. Estimating mixed memberships with sharp eigenvector deviations. *Journal of the American Statistical Association*, pages 1–13, 2020.
- F. McSherry. Spectral partitioning of random graphs. In *Proceedings 2001 IEEE International Conference on Cluster Computing*, pages 529–537, 2001.
- Mark EJ Newman. The structure of scientific collaboration networks. *Proceedings of the national academy of sciences*, 98(2):404–409, 2001.
- Mark EJ Newman. Finding community structure in networks using the eigenvectors of matrices. *Physical review E*, 74(3):036104, 2006.
- Tin Lok James Ng and Thomas Brendan Murphy. Weighted stochastic block model. *Statistical Methods and Applications*, 2021.
- John Palowitch, Shankar Bhamidi, and Andrew B. Nobel. Significance-based community detection in weighted networks. *Journal of Machine Learning Research*, 18(188):1–48, 2018.
- Symeon Papadopoulos, Yiannis Kompatsiaris, Athena Vakali, and Ploutarchos Spyridonos. Community detection in social media. *Data mining and knowledge discovery*, 24(3):515–554, 2012.
- Huan Qing. Distribution-free models for community detection. *arXiv preprint arXiv:2111.07495*, 2021.
- Huan Qing. A useful criterion on studying consistent estimation in community detection. *Entropy*, 24(8):1098, 2022a.
- Huan Qing. Degree-corrected distribution-free model for community detection in weighted networks. *Scientific Reports*, 12(1):1–19, 2022b.
- Kenneth E Read. Cultures of the central highlands, new guinea. *Southwestern Journal of Anthropology*, 10(1):1–43, 1954.
- Karl Rohe, Sourav Chatterjee, and Bin Yu. Spectral clustering and the high-dimensional stochastic blockmodel. *Annals of Statistics*, 39(4):1878–1915, 2011.
- Joel A. Tropp. User-friendly tail bounds for sums of random matrices. *Foundations of Computational Mathematics*, 12(4):389–434, 2012.
- Zhe. Wang, Yingbin. Liang, and Pengsheng. Ji. Spectral algorithms for community detection in directed networks. *Journal of Machine Learning Research*, 21:1–45, 2020.
- Jierui Xie, Stephen Kelley, and Boleslaw K Szymanski. Overlapping community detection in networks: The state-of-the-art and comparative study. *Acm computing surveys (csur)*, 45(4):1–35, 2013.
- Min Xu, Varun Jog, and Po-Ling Loh. Optimal rates for community estimation in the weighted stochastic block model. *Annals of Statistics*, 48(1):183–204, 2020.
- Bo Yang, William Cheung, and Jiming Liu. Community mining from signed social networks. *IEEE transactions on knowledge and data engineering*, 19(10):1333–1348, 2007.
- Wayne W Zachary. An information flow model for conflict and fission in small groups. *Journal of anthropological research*, 33(4):452–473, 1977.
- Yuan Zhang, Elizaveta Levina, and Ji Zhu. Detecting overlapping communities in networks using spectral methods. *SIAM Journal on Mathematics of Data Science*, 2(2):265–283, 2020.

Yunpeng Zhao, Elizaveta Levina, and Ji Zhu. Consistency of community detection in networks under degree-corrected stochastic block models. *Annals of Statistics*, 40(4):2266–2292, 2012.

Zhixin Zhou and Arash A.Amini. Analysis of spectral clustering algorithms for community detection: the general bipartite setting. *Journal of Machine Learning Research*, 20(47):1–47, 2019.

Appendix A. Vertex hunting algorithm

Algorithm 2 is the SP algorithm.

Algorithm 2 Successive Projection (SP) Gillis and Vavasis (2015)

Require: Near-separable matrix $Y_{sp} = S_{sp}M_{sp} + Z_{sp} \in \mathbb{R}_+^{m \times n}$, where S_{sp}, M_{sp} should satisfy Assumption 1 Gillis and Vavasis (2015), the number r of columns to be extracted.

Ensure: Set of indices \mathcal{K} such that $Y_{sp}(\mathcal{K}, :) \approx S$ (up to permutation)

- 1: Let $R = Y_{sp}, \mathcal{K} = \{\}$, $k = 1$.
 - 2: **While** $R \neq 0$ and $k \leq r$ **do**
 - 3: $k_* = \operatorname{argmax}_k \|R(k, :)\|_F$.
 - 4: $u_k = R(k_*, :)$.
 - 5: $R \leftarrow (I - \frac{u_k u_k'}{\|u_k\|_F^2})R$.
 - 6: $\mathcal{K} = \mathcal{K} \cup \{k_*\}$.
 - 7: $k = k + 1$.
 - 8: **end while**
-

Appendix B. Proofs under MMDF

B.1 Proof of Proposition 1

Proof By Lemma 1, under MMDF, $U = \Pi B = \Pi U(\mathcal{I}, :)$ gives $\Pi U(\mathcal{I}, :) = \tilde{\Pi} U(\mathcal{I}, :)$ since $\Omega = \rho \Pi P \Pi' = \rho \tilde{\Pi} \tilde{P} \tilde{\Pi}' = U \Lambda U'$. Since $\operatorname{rank}(P) = \operatorname{rank}(\tilde{P}) = \operatorname{rank}(\Pi) = \operatorname{rank}(\tilde{\Pi}) = K$ and $B \in \mathbb{R}^{K \times K}$, we have $\operatorname{rank}(B) = K$ and the inverse of B exists. Therefore $\Pi B = \tilde{\Pi} B$ gives $\Pi = \tilde{\Pi}$. Since $\Omega(\mathcal{I}, \mathcal{I}) = \rho \Pi(\mathcal{I}, :) P \Pi'(\mathcal{I}, :) = \rho P = \rho \tilde{\Pi}(\mathcal{I}, :) \tilde{P} \tilde{\Pi}'(\mathcal{I}, :) = \rho \Pi(\mathcal{I}, :) \tilde{P} \Pi'(\mathcal{I}, :) = \rho \tilde{P}$, we have $P = \tilde{P}$, and this proposition follows. \blacksquare

B.2 Proof of Lemma 1

Proof Since $\Omega = \Pi \rho P \Pi' = U \Lambda U'$ and $U'U = I_K$, we have $U = \Pi \rho P \Pi' U \Lambda^{-1}$, i.e., $B = \rho P \Pi' U \Lambda^{-1}$. So B is unique. Since $U = \Pi B$, we have $U(\mathcal{I}, :) = \Pi(\mathcal{I}, :) B = B$ and the lemma follows. \blacksquare

B.3 Proof of Lemma 2

Proof First, we use Theorem 1.4 (the Matrix Bernstein) of Tropp (2012) to build an upper bound on $\|A - \Omega\|_\infty$. This theorem is given below

Theorem 2 Consider a finite sequence $\{X_k\}$ of independent, random, self-adjoint matrices with dimension d . Assume that each random matrix satisfies

$$\mathbb{E}[X_k] = 0, \text{ and } \|X_k\| \leq R \text{ almost surely.}$$

Then, for all $t \geq 0$,

$$\mathbb{P}\left(\left\|\sum_k X_k\right\| \geq t\right) \leq d \cdot \exp\left(\frac{-t^2/2}{\sigma^2 + Rt/3}\right),$$

where $\sigma^2 := \|\sum_k \mathbb{E}(X_k^2)\|$.

Let $x = (x_1, x_2, \dots, x_n)'$ be any $n \times 1$ vector. For any $i, j \in [n]$, we have $\mathbb{E}[(A(i, j) - \Omega(i, j))x(j)] = 0$ and $\|(A(i, j) - \Omega(i, j))x(j)\| \leq \tau \|x\|_\infty$ by Assumption 1. Set $R = \tau \|x\|_\infty$, a finite value by Assumption 1. Since $\|\sum_{j=1}^n \mathbb{E}[(A(i, j) - \Omega(i, j))^2 x^2(j)]\| = \|\sum_{j=1}^n x^2(j) \mathbb{E}[(A(i, j) - \Omega(i, j))^2]\| = \|\sum_{j=1}^n x^2(j) \text{Var}(A(i, j))\| \leq \gamma \rho \sum_{j=1}^n x^2(j)$ where the last inequality holds by Assumption 1, by Theorem 2, for any $t \geq 0$ and $i \in [n]$, we have

$$\mathbb{P}(|\sum_{j=1}^n (A(i, j) - \Omega(i, j))x(j)| > t) \leq 2 \exp(-\frac{t^2/2}{\gamma \rho \sum_{j=1}^n x^2(j) + \frac{Rt}{3}}).$$

Set $x(j)$ as 1 or -1 such that $(A(i, j) - \Omega(i, j))y(j) = |A(i, j) - \Omega(i, j)|$, we have

$$\mathbb{P}(\|A - \Omega\|_\infty > t) \leq 2 \exp(-\frac{t^2/2}{\gamma \rho n + \frac{Rt}{3}}).$$

Set $t = \frac{\alpha+1+\sqrt{(\alpha+1)(\alpha+19)}}{3} \sqrt{\gamma \rho n \log(n)}$ for any $\alpha > 0$. By assumption 2, we have

$$\mathbb{P}(\|A - \Omega\|_\infty > t) \leq 2 \exp(-\frac{t^2/2}{\gamma \rho n + \frac{Rt}{3}}) \leq n^{-\alpha}.$$

By Theorem 4.2 of Cape et al. (2019), when $\sigma_K(\Omega) \geq 4\|A - \Omega\|_\infty$, we have

$$\|\hat{U} - U\mathcal{O}\|_{2 \rightarrow \infty} \leq 14 \frac{\|A - \Omega\|_\infty}{\sigma_K(\Omega)} \|U\|_{2 \rightarrow \infty},$$

where \mathcal{O} is a $K \times K$ orthogonal matrix. With probability at least $1 - o(n^{-\alpha})$, we have

$$\|\hat{U} - U\mathcal{O}\|_{2 \rightarrow \infty} = O(\frac{\|U\|_{2 \rightarrow \infty} \sqrt{\gamma \rho n \log(n)}}{\sigma_K(\Omega)}).$$

Since $\hat{U}'\hat{U} = I_K, U'U = I_K$, by basic algebra, we have $\|\hat{U}\hat{U}' - UU'\|_{2 \rightarrow \infty} \leq 2\|\hat{U} - U\mathcal{O}\|_{2 \rightarrow \infty}$, which gives

$$\|\hat{U}\hat{U}' - UU'\|_{2 \rightarrow \infty} = O(\frac{\|U\|_{2 \rightarrow \infty} \sqrt{\gamma \rho n \log(n)}}{\sigma_K(\Omega)}).$$

Since $\sigma_K(\Omega) \geq \sigma_K(P) \rho \lambda_K(\Pi'\Pi)$ by Lemma II.4 of Mao et al. (2020) and $\|U\|_{2 \rightarrow \infty}^2 \leq \frac{1}{\lambda_K(\Pi'\Pi)}$ by Lemma 3.1 of Mao et al. (2020), where this two lemmas are distribution-free and always hold as long as Equations (2), (4) and (5) hold, we have

$$\|\hat{U}\hat{U}' - UU'\|_{2 \rightarrow \infty} = O(\frac{\sqrt{\gamma n \log(n)}}{\sigma_K(P) \rho^{0.5} \lambda_K^{1.5}(\Pi'\Pi)}).$$

Set $\alpha = 3$, and this claim follows. ■

B.4 Proof of Theorem 1

Proof Since DFSP is the SPACL algorithm without the prune step of Mao et al. (2020), the proof of DFSP's consistency is the same as SPACL except for the row-wise eigenspace error step where we need to consider γ which is directly related with distribution \mathcal{F} . By Eq (3) in Theorem 3.2 of Mao et al. (2020) where the proof is distribution-free, there exists a $K \times K$ permutation matrix \mathcal{P} such that

$$\max_{i \in [n]} \|e'_i(\hat{\Pi} - \Pi\mathcal{P})\|_1 = O(\varpi \kappa(\Pi'\Pi) \sqrt{\lambda_1(\Pi'\Pi)}).$$
■

B.5 Proof of Corollary 1

Proof When $\lambda_K(\Pi'\Pi) = O(\frac{n}{K})$ and $K = O(1)$, we have $\max_{i \in [n]} \|e'_i(\hat{\Pi} - \Pi\mathcal{P})\|_1 = O(\varpi\sqrt{n})$ by Theorem 1, and $\varpi = O(\frac{1}{\sigma_K(P)} \frac{1}{\sqrt{n}} \sqrt{\frac{\gamma \log(n)}{\rho n}})$ by Lemma 2. Then the corollary follows immediately. ■